Rapid Communications

Impact of piezoelectric fields on coherent zone-folded phonons in GaAs/AlAs superlattices

Felix Mahler [1], Klaus Reimann [1], Michael Woerner [1], Thomas Elsaesser [1], Christos Flytzanis [2] and Klaus Biermann [3]
[1] *Max-Born-Institut für Nichtlineare Optik und Kurzzeitspektroskopie, 12489 Berlin, Germany*
[2] *Laboratoire de Physique, École Normale Supérieure, Université PSL, 75231 Paris, France*
[3] *Paul-Drude-Institut für Festkörperelektronik, 10117 Berlin, Germany*

(Received 27 June 2019; revised manuscript received 4 September 2019; published 12 September 2019)

The amplitude decay of folded longitudinal acoustic phonon oscillations in GaAs/AlAs superlattices grown in the [100] and [111] directions is studied as a function of carrier excitation density. Time-resolved pump-probe measurements in reflection reveal decay times on the order of several tens of picoseconds, which are independent of the excitation density for all phonons in the [100] sample and for phonons at wave vectors $q \neq 0$ in the [111] sample. In contrast, the decay time increases with carrier density for the phonon at $q = 0$ in the [111] sample. This phonon couples to the photoexcited electron-hole plasma via the piezoelectric interaction. Friction in the carrier plasma induces a damping of the phonon oscillations. The impact of the piezoelectric phonon-electron coupling on the amplitude decay is reduced by screening at high carrier density, resulting in longer phonon decay times.

DOI: 10.1103/PhysRevB.100.121302

Introduction. Semiconductor superlattices [1] have attracted attention for the generation and amplification of sound waves with ultrahigh frequencies up to the terahertz range [2–8]. While it is possible to optically excite either acoustic phonons with low frequencies or optical phonons with high frequencies in bulk semiconductors, the phonon spectrum of superlattices can be tailored by design, e.g., by exploiting the occurrence of backfolded acoustic phonons.

A superlattice consists of a periodic arrangement of layers of two different materials. In the direction normal to the layers, it represents an artificial crystal with a lattice constant much larger than those of the layer materials. Accordingly, the Brillouin zone along this direction extends only from $-\pi/d$ to π/d (d is the superlattice period), which is a small part of the bulk Brillouin zone. This leads to a backfolding of all states in the bulk material into the superlattice Brillouin zone, resulting in a strong increase of the number of phonon branches that can be excited optically [2]. The generation, propagation, damping, and amplification of coherent superlattice phonons have been studied in detail, including measurements of their mean free path upon propagation into bulk semiconductor substrates [3–23].

Coherent superlattice phonons have been generated with femtosecond pulses at photon energies in the range of the superlattice band gap. Both displacive excitation via the mechanical stress originating from the generation and subsequent relaxation of a photoexcited electron-hole plasma, and resonantly enhanced impulsive Raman scattering within the spectrum of the pump pulses have been exploited. In the presence of an electron-hole plasma, coherent phonons couple to carriers via different types of electron-phonon interactions, making the coherent phonon amplitude susceptible to carrier dynamics, e.g., friction in the carrier system and/or transient charge transport. In polar zinc-blende semiconductors such as GaAs and AlAs, the relevant electron-phonon interaction terms depend on the orientation of the superlattice, i.e., on the growth direction. For longitudinal superlattice phonons in the [100] direction, electron-phonon coupling arises only via the deformation-potential interaction, whereas in the [111] direction one has the piezoelectric interaction on top [24,25]. While Raman spectra of phonons at wave vectors $q \neq 0$ have been studied in a [311] superlattice with a built-in piezoelectric field [26], the influence of piezoelectric coupling on the decay of coherent phonon excitations has remained mainly unexplored.

In the present Rapid Communication, we investigate the influence of the piezoelectric interaction on coherent folded phonons in time-resolved optical pump-probe experiments with femtosecond pulses. Phonon kinetics are mapped by the transient modulation of the optical reflectivity of the superlattice samples. We compare two (otherwise identical) GaAs/AlAs superlattices grown in the [100] and [111] directions and demonstrate the distinct and strong influence of piezoelectric coupling on phonon decays in the [111] sample.

Experiment. The two superlattice samples were grown by molecular beam epitaxy on 350-μm-thick n-doped substrates. They each contain 70 periods of GaAs quantum wells of a thickness of $d_1 = 9.7$ nm and AlAs barriers with $d_2 = 1.5$ nm (period $d = d_1 + d_2 = 11.2$ nm). The GaAs layers are n doped with a sheet density of 6×10^9 cm^{-2}. On top of the superlattice structures are 55-nm-thick n-doped GaAs cap layers. Room-temperature photoluminescence measurements indicate that the first interband transition energy is around 1.47 eV for both samples.

Pump-probe measurements were carried out with a mode-locked Ti:sapphire oscillator (Spectra-Physics Tsunami), having a center photon energy of 1.5 eV, a spectral bandwidth of 45 meV [full width at half maximum (FWHM)], a pulse length of 80 fs, and a repetition rate of 80 MHz. At this photon energy the absorption length is about 1 μm [27], so that electron-hole pairs are generated in all GaAs layers of the superlattices.

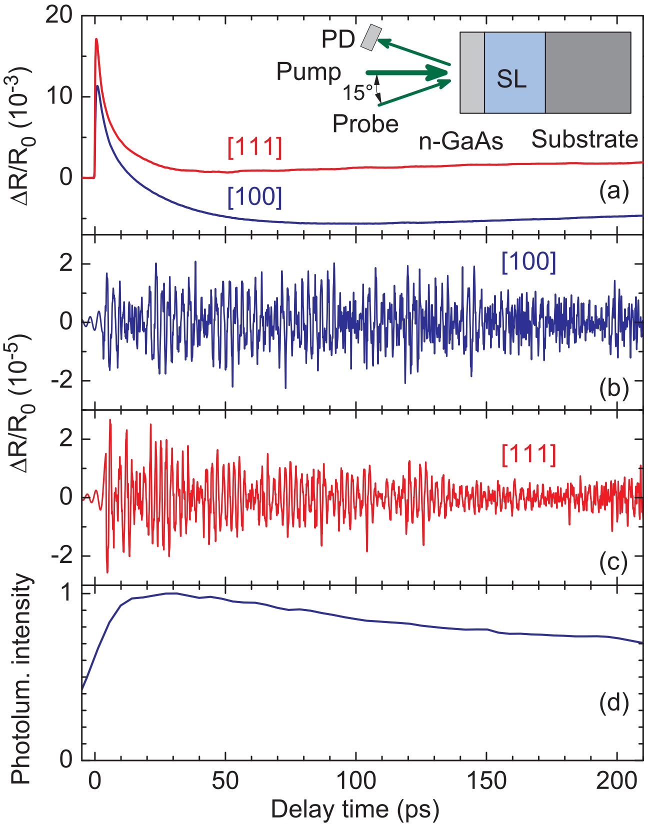

FIG. 1. (a) Transients of the reflectivity change of the [100] sample (blue) and the [111] sample (red). The reflectivity change $\Delta R/R_0 = (R - R_0)/R_0$ is plotted as a function of pump-probe delay (R, R_0: reflectivity with and without excitation). The energy of the pump pulse was 9.5 nJ. (b), (c) Oscillatory components of the transients in (a) after subtraction of a ratelike background kinetics. (d) Kinetics of spectrally integrated superlattice photoluminescence (25 ps time resolution) from the [100] sample. The recombination time of 0.9 ns is much longer than the decay times of the coherent phonon amplitudes shown in Fig. 3(a).

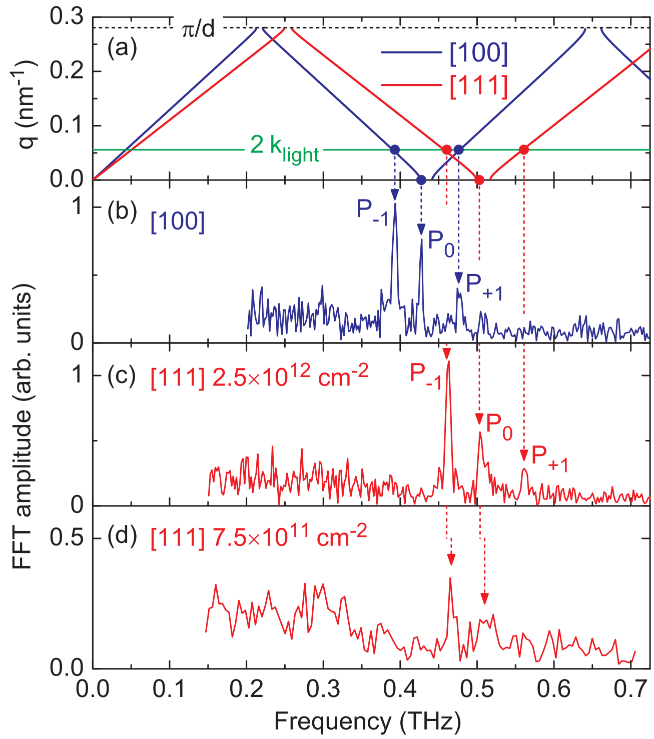

FIG. 2. (a) Calculated dispersion curves of folded longitudinal acoustic phonons for the two growth directions. (b), (c) Spectra of the oscillatory signals from Figs. 1(b) and 1(c). (d) Same as in (c), but for a lower carrier density. The dashed arrows connect the observed peaks to the dispersion curves.

Pump and probe pulses were linearly polarized with the probe perpendicular to the pump.

The experimental geometry is sketched in the inset of Fig. 1(a). Both pump and probe pulses were focused onto the sample with a spot diameter of 70 μm (FWHM). The pump energy was varied between 0.85 nJ corresponding to a two-dimensional electron-hole pair density of 2.2×10^{11} cm^{-2}, and 9.5 nJ (2.5×10^{12} cm^{-2}). The energy of the probe pulse was kept constant at 90 pJ. The pump beam was incident normal to the surface and mechanically chopped at a frequency of 1630 Hz for lock-in detection (Stanford Research SR830) of the pump-probe signals. The probe beam was incident under an angle of 15° for spatial separation from the pump. The reflected probe pulses were detected with a Si photodiode (Thorlabs DET36A). In addition to the spatial separation, a polarizer in front of the photodiode reduced scattered pump light to a negligible level. All measurements were performed at room temperature with the samples mounted on a copper heat sink.

Results. Figure 1(a) shows the time-dependent reflectivity changes of the [100] and [111] samples for a pump pulse energy of 9.5 nJ. In both samples the reflectivity rises within our time resolution. The subsequent decays extends over some 100 ps and follows an incoherent, i.e., ratelike kinetics. This behavior reflects relaxation processes and real-space transfer of photoexcited carriers in the superlattice and in the cap layer and will not be analyzed in the present context. We would like to stress that the signal does *not* directly give the carrier density. The latter decays on a nanosecond timescale, as is evident from the time-resolved decay of photoluminescence [Fig. 1(d); see also Refs. [28–30]].

Superimposed on the incoherent kinetics are the (much weaker) oscillatory phonon signals, which are the subject of the present Rapid Communication. To extract the oscillating component from the pump-probe transients, a triexponential fit of the incoherent decays is subtracted from the full data. The resulting difference data are high-pass filtered with a cutoff frequency of 0.1 THz. This procedure results in the oscillatory time-dependent phonon transients presented in Figs. 1(b) and 1(c). The frequency-domain spectra of such signals as determined by Fourier transform are displayed in Figs. 2(b) and 2(c). Both samples show three main frequency components in the range between 0.3 and 0.6 THz.

In Fig. 2(a), we compare the frequency positions of the observed peaks (labeled P_{-1}, P_0, P_{+1}) with dispersion curves for zone-folded longitudinal acoustic phonons, calculated with the elastic continuum model [31–33]. The difference between the phonon dispersions in the two samples is caused by the higher speed of sound in the [111] direction compared to the

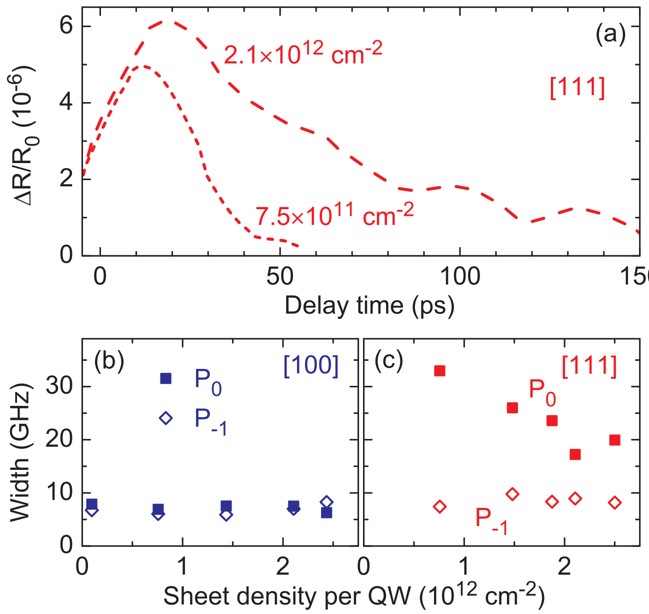

FIG. 3. (a) Envelopes of the P_0 oscillation at 510 GHz in the [111] sample at two different carrier densities. A much faster decrease is observed at lower carrier densities. (b), (c) Corresponding linewidths (FWHM) as a function of carrier density.

[100] direction. For both samples, the peaks P_{-1} and P_{+1} are identified as folded phonons at $q = 2k_{\rm light}$ [34] and peak P_0 as the folded phonon at $q = 0$. The excitation mechanisms for these folded phonons are impulsive Raman scattering [3,9,26,35] and displacive excitation [6,36,37] due to the photoexcited electron-hole pairs in the GaAs quantum wells. Selecting the P_0 peak (by a frequency filter) and transforming it back to the time domain gives the time-dependent envelopes shown in Fig. 3(a) for two different excitation densities of the [111] sample. The decay of such envelopes slows down for higher excitation densities but is much faster than carrier recombination [cf. Fig. 1(d)], i.e., there are only minor changes of carrier concentration during the envelope decays.

Apart from the higher frequencies for the [111] direction because of the higher speed of sound, the spectra in Figs. 2(b) and 2(c) taken with 9.5 nJ pump energy display the same pattern of phonon lines. We now consider the spectral widths of the individual Fourier components. The spectral widths (FWHM) of the peaks from the [100] sample are plotted as a function of the carrier sheet density per quantum well in Fig. 3(b). They are independent of carrier density, as is the width of the P_{-1} peak from the [111] sample [Fig. 3(c)]. In contrast, the width of its P_0 component *decreases* with increasing carrier density [Figs. 2(c) and 2(d)], a behavior which is in line with the slowing down of the decay of the P_0 envelope [Fig. 3(a)]. This surprising observation is opposite to the behavior of optical phonons in bulk GaAs, for which the decay of the temporal envelope becomes faster, i.e., the linewidth *increases*, for increasing excitation density [38]. It should be noted that the frequency positions of all peaks in our measurements are independent of pump energy [apart from a small overall shift caused by sample heating; cf. Figs. 2(c) and 2(d)].

Discussion. The mechanisms for the femtosecond excitation of backfolded superlattice phonons have been analyzed in the extensive literature [2–6,21,36,39–41] and will not be reconsidered here. Instead, we focus on the unexpected behavior of the P_0 phonons in the [111] sample, namely, the decreasing linewidth of the Fourier spectra [Fig. 3(c)] and slowing down of the picosecond envelope decay [Fig. 3(a)] with increasing carrier density.

The elastic continuum model [31–33] leads to the following equation for a plane wave in the z direction in a homogeneous material,

$$\rho_\alpha \frac{\partial^2}{\partial z^2} u(z,t) = C_\alpha \frac{\partial^2}{\partial t^2} u(z,t). \tag{1}$$

Here, ρ_α is the density of material α, C_α the relevant elastic constant (for longitudinal acoustic waves in the [100] direction $C = c_{11}$, for the [111] direction $3C = c_{11} + 2c_{12} + 4c_{44}$ [42]), and $u(z,t)$ the displacement from the equilibrium position. The speed of sound v_α follows from Eq. (1) as $v_\alpha = \sqrt{C_\alpha/\rho_\alpha}$. For the calculation of the phonon dispersion we use the following parameters: $c_{11} = 1.19 \times 10^{11}$ N/m^2, $c_{12} = 5.38 \times 10^{10}$ N/m^2, $c_{44} = 5.95 \times 10^{10}$ N/m^2, $\rho = 5317$ kg/m^3 [43] for GaAs and $c_{11} = 1.2 \times 10^{11}$ N/m^2, $c_{12} = 5.7 \times 10^{10}$ N/m^2, $c_{44} = 5.9 \times 10^{10}$ N/m^2, $\rho = 3760$ kg/m^3 [44] for AlAs.

At the boundary of two materials, both the displacement and the stress have to be continuous, leading for a boundary at $z = 0$ to [31,33]

$$u(0+\delta,t) = u(0-\delta,t), \quad d \gg \delta > 0, \tag{2}$$

$$C_1 \frac{\partial}{\partial z} u(0+\delta,t) = C_2 \frac{\partial}{\partial z} u(0-\delta,t). \tag{3}$$

With the requirement for a wave with wave vector q,

$$u(z+d,t) = \exp(iqd)u(z,t), \tag{4}$$

this results in the dispersion curves of Fig. 2(a), the displacements of Fig. 4(a), and the strain $s(z,t) = \partial u(z,t)/\partial z$ of Fig. 4(b). The observed phonon frequencies agree for both growth directions with the calculations.

The connection between the strain components s_{jk} and the generated electric polarization $\mathbf{P}$ is given by the piezoelectric tensor e_{ijk} [42],

$$P_i = \sum_{jk} e_{ijk} s_{jk} \quad (i,j,k = x,y,z). \tag{5}$$

In crystals with a zinc-blende structure, the only nonzero coefficient is $e_{xyz} = e_{yzx} = e_{zxy} = e_{xzy} = e_{yxz} = e_{zyx}$ [45,46]. A strain along the [100] direction, which is equivalent to a longitudinal acoustic phonon in this direction, does not generate a piezoelectric polarization. In contrast, a strain along [111] leads to a longitudinal piezoelectric polarization parallel to [111]. Accordingly, a longitudinal acoustic phonon propagating in the [111] direction couples to the electrons by the piezoelectric and deformation potential interaction, whereas a longitudinal acoustic phonon propagating in the [100] direction couples via the deformation potential only [24,25].

The strain and the related piezoelectric polarization have, at a fixed time, only for $q = 0$ the same value in different

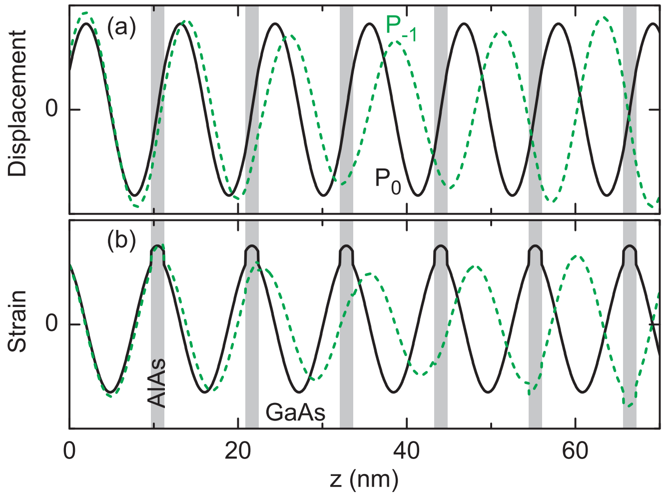

FIG. 4. (a) Displacement of the modes P_{-1} (dashed green line) and P_0 (solid black line). (b) Corresponding strain. While both the displacement and the stress are continuous at the layer boundaries [Eqs. (2) and (3)], the strain exhibits jumps because of the different elastic constants. The displacement and the strain look identical for longitudinal folded phonons in both directions, [100] and [111], but the strain generates a piezoelectric polarization only in the [111] direction.

periods of the superlattice [cf. Fig. 4(b) and Eq. (4)]. For $q \neq 0$, the piezoelectric polarization is positive in some layers and negative in other layers, so that its average over many superlattice periods is zero. This average is relevant for the influence on the electrons since in a superlattice the electron wave functions are delocalized over many periods [47]. A macroscopic electric polarization exists only for the peak P_0 at $q = 0$ in the [111] sample and oscillates with the frequency of the P_0 mode. The related macroscopic electric field couples to the photogenerated electron-hole plasma via the piezoelectric interaction [45] which is particularly strong for small q, i.e., for the P_0 mode. Carrier oscillations induced via the oscillating piezoelectric field are strongly damped by friction mainly due to inelastic scattering processes in the electron-hole plasma. As a result of the piezoelectric interaction, friction in the carrier plasma acts back on the coherent phonon motions and leads to the damping of the envelopes of Fig. 3(a). During this process, the carrier density undergoes only minor changes [Fig. 1(d)].

The linewidths of the P_0 peak [Fig. 3(c)] are substantially higher than those of the P_{-1} peak. We assign this extra width to the damping of the coherent phonon amplitude by the piezoelectric interaction with the electron-hole plasma. The P_{-1} peak displays a spectral width (FWHM) of $\Delta\nu =$ 7 GHz, similar to the peaks measured with the [100] sample [Fig. 3(b)]. For a predominant homogeneous broadening, this $\Delta\nu$ translates into a dephasing time of $T_2^0 = 46$ ps. The [111] P_0 peak has a spectral width of approximately 28 GHz for a carrier density of 7.5×10^{11} cm^{-2}, corresponding to $T_2 =$ 11.4 ps. According to $\tau^{-1} = (T_2)^{-1} - (T_2^0)^{-1}$, one estimates a time constant of additional damping of $\tau \approx 15$ ps, in good agreement with the damping of the corresponding envelope in Fig. 3(a). For a carrier density of 2.1×10^{12} cm^{-2}, a value of $\tau \approx 40$ ps is derived, similar to the envelope decay time.

The damping of the coherent P_0 phonon oscillations becomes less efficient with increasing density of the photoexcited electron-hole plasma. This behavior is due to a weakening of the piezoelectric interaction by electric screening. For low carrier densities, the piezoelectric interaction is strongest and results in a strong damping of the coherent phonon motions. At high electron-hole densities, screening limits the impact of friction on the phonon motions, leading to a weaker damping. We estimated the characteristic screening lengths from a standard Thomas-Fermi approach for a quasi-two-dimensional carrier system [48]. For a sheet density of 2×10^{11} cm^{-2}, the screening length $\kappa^{-1} = 20$ nm, which is longer than the superlattice period of our samples of 11.2 nm. In contrast, a screening length $\kappa^{-1} = 5$ nm, about half the superlattice period, is calculated for a sheet density of 2.5×10^{12} cm^{-2}, resulting in less damping and a smaller linewidth of the P_0 spectrum.

A microscopic theory of phonon damping via the piezoelectric coupling needs to be developed. Vertical carrier transport through the superlattice in response to the phonon-induced electric field, which is the main source of phonon damping, is a very complex phenomenon. The driving field is spatially inhomogeneous, i.e., mainly located in the barriers as the strain profiles in Fig. 4 suggest. Thus, in addition to the electric-field screening discussed above, the vertical carrier transport contains spatially nonlocal contributions, making a transport theory very demanding. Thus, we refrain from an attempt to quantitatively calculate the phonon damping.

Conclusions. A comparative pump-probe study of [100] and [111] GaAs/AlAs superlattices has demonstrated the influence of piezoelectric phonon-electron interactions on the amplitude decay of coherent zone-folded phonons. A macroscopic piezoelectric field couples the coherent phonon motions to a photoexcited electron-hole plasma which introduces friction and, thus, damping of the coherent phonon amplitudes. At two-dimensional carrier densities of some 10^{12} cm^{-2} the piezoelectric field gets screened, reducing the piezoelectric damping term. Our results are relevant for acoustic wave resonators made from polar semiconductors [23,35]. The damping mechanism established here directly affects the quality factor of such resonators. Beyond those applications, our study is a step towards understanding the decay of the coherent phonon amplitude in piezoelectric materials in general.

Acknowledgment. The authors acknowledge the support of Günter Steinmeyer with the experimental setup.

[1] L. Esaki and R. Tsu, Superlattice and negative differential conductivity in semiconductors, IBM J. Res. Dev. **14**, 61 (1970).

[2] C. Colvard, R. Merlin, M. V. Klein, and A. C. Gossard, Observation of Folded Acoustic Phonons in a Semiconductor Superlattice, Phys. Rev. Lett. **45**, 298 (1980).

[3] A. Bartels, T. Dekorsy, H. Kurz, and K. Köhler, Coherent Zone-Folded Longitudinal Acoustic Phonons in Semiconductor Superlattices: Excitation and Detection, Phys. Rev. Lett. **82**, 1044 (1999).

[4] K. Mizoguchi, M. Hase, S. Nakashima, and M. Nakayama, Observation of coherent folded acoustic phonons propagating in a GaAs/AlAs superlattice by two-color pump-probe spectroscopy, Phys. Rev. B **60**, 8262 (1999).

[5] R. P. Beardsley, A. V. Akimov, M. Henini, and A. J. Kent, Coherent Terahertz Sound Amplification and Spectral Line Narrowing in a Stark Ladder Superlattice, Phys. Rev. Lett. **104**, 085501 (2010).

[6] K. Shinokita, K. Reimann, M. Woerner, T. Elsaesser, R. Hey, and C. Flytzanis, Strong Amplification of Coherent Acoustic Phonons by Intraminiband Currents in a Semiconductor Superlattice, Phys. Rev. Lett. **116**, 075504 (2016).

[7] A. Yamamoto, T. Mishina, Y. Masumoto, and M. Nakayama, Coherent Oscillation of Zone-Folded Phonon Modes in GaAs-AlAs Superlattices, Phys. Rev. Lett. **73**, 740 (1994).

[8] A. J. Kent, R. N. Kini, N. M. Stanton, M. Henini, B. A. Glavin, V. A. Kochelap, and T. L. Linnik, Acoustic Phonon Emission from a Weakly Coupled Superlattice Under Vertical Electron Transport: Observation of Phonon Resonance, Phys. Rev. Lett. **96**, 215504 (2006).

[9] B. Jusserand, D. Paquet, F. Mollot, F. Alexandre, and G. Le Roux, Influence of the supercell structure on the folded acoustical Raman line intensities in superlattices, Phys. Rev. B **35**, 2808 (1987).

[10] M. Holtz, K. Syassen, and K. Ploog, Folded-acoustic phonons in GaAs/AlAs thin-layer superlattices under high pressure, Phys. Rev. B **40**, 2988 (1989).

[11] M. Holtz, K. Syassen, U. D. Venkateswaran, K. Ploog, and R. Muralidharan, High pressure Raman studies of GaAs/AlAs superlattices: Folded acoustic phonons and resonant second-order scattering, High Press. Res. **3**, 245 (1990).

[12] R. Fukasawa, Y. Okubo, O. Abe, and K. Ohta, Raman scattering spectra of the folded acoustic phonon in $Al_xGa_{1-x}As$/GaAs superlattices for various Al mole fractions, Jpn. J. Appl. Phys. **31**, 816 (1992).

[13] K. Mizoguchi, H. Takeuchi, T. Hino, and M. Nakayama, Finite-size effects on coherent folded acoustic phonons in GaAs/AlAs superlattices, J. Phys.: Condens. Matter **14**, L103 (2002).

[14] D. C. Heinecke, O. Kliebisch, J. Flock, A. Bruchhausen, K. Köhler, and T. Dekorsy, Selective excitation of zone-folded phonon modes within one triplet in a semiconductor superlattice, Phys. Rev. B **87**, 075307 (2013).

[15] Z. V. Popović, M. Cardona, E. Richter, D. Strauch, L. Tapfer, and K. Ploog, Phonons in GaAs/AlAs superlattices grown along the [111] direction, Phys. Rev. B **41**, 5904 (1990).

[16] C.-K. Sun, J.-C. Liang, and X.-Y. Yu, Coherent Acoustic Phonon Oscillations in Semiconductor Multiple Quantum Wells with Piezoelectric Fields, Phys. Rev. Lett. **84**, 179 (2000).

[17] Ü. Özgür, C.-W. Lee, and H. O. Everitt, Control of Coherent Acoustic Phonons in Semiconductor Quantum Wells, Phys. Rev. Lett. **86**, 5604 (2001).

[18] Y.-C. Wen, L.-C. Chou, H.-H. Lin, V. Gusev, K.-H. Lin, and C.-K. Sun, Efficient generation of coherent acoustic phonons in (111) InGaAs/GaAs multiple quantum wells through piezoelectric effects, Appl. Phys. Lett. **90**, 172102 (2007).

[19] C. Aku-Leh, K. Reimann, M. Woerner, E. Monroy, and D. Hofstetter, Coupling of intersubband transitions to zone-folded acoustic phonons in a GaN/AlN superlattice, Phys. Rev. B **85**, 155323 (2012).

[20] R. Legrand, A. Huynh, B. Jusserand, B. Perrin, and A. Lemaître, Direct measurement of coherent subterahertz acoustic phonons mean free path in GaAs, Phys. Rev. B **93**, 184304 (2016).

[21] P. Ruello and V. E. Gusev, Physical mechanisms of coherent acoustic phonons generation by ultrafast laser action, Ultrasonics **56**, 21 (2015).

[22] M. Trigo, T. A. Eckhause, M. Reason, R. S. Goldman, and R. Merlin, Observation of Surface-Avoiding Waves: A New Class of Extended States in Periodic Media, Phys. Rev. Lett. **97**, 124301 (2006).

[23] M. F. Pascual Winter, G. Rozas, A. Fainstein, B. Jusserand, B. Perrin, A. Huynh, P. O. Vaccaro, and S. Saravanan, Selective Optical Generation of Coherent Acoustic Nanocavity Modes, Phys. Rev. Lett. **98**, 265501 (2007).

[24] B. K. Ridley, Hot electrons in low-dimensional structures, Rep. Prog. Phys. **54**, 169 (1991).

[25] B. K. Ridley, *Quantum Processes in Semiconductors*, 3rd ed. (Oxford University Press, Oxford, UK, 1993).

[26] G. Rozas, M. F. Pascual Winter, A. Fainstein, B. Jusserand, P. O. Vaccaro, and S. Saravanan, Acoustic phonon Raman scattering induced by a built-in electric field, Phys. Rev. B **77**, 165314 (2008).

[27] J. H. C. Casey, D. D. Sell, and K. W. Wecht, Concentration dependence of the absorption coefficient for *n*- and *p*-type GaAs between 1.3 and 1.6 eV, J. Appl. Phys. **46**, 250 (1975).

[28] Y. Arakawa, H. Sakaki, M. Nishioka, J. Yoshino, and T. Kamiya, Recombination lifetime of carriers in GaAs-GaAlAs quantum wells near room temperature, Appl. Phys. Lett. **46**, 519 (1985).

[29] J. Christen and D. Bimberg, Recombination dynamics of carriers in GaAs-GaAlAs quantum well structures, Surf. Sci. **174**, 261 (1986).

[30] A. Werner, M. Kunst, G. Beck, J. Christen, and G. Weimann, Charge-carrier dynamics in GaAs multiple quantum wells determined by contactless photoconductivity measurements, Phys. Rev. B **34**, 5918 (1986).

[31] S. M. Rytov, Acoustical properties of a thinly laminated medium, Akust. Zh. **2**, 71 (1956) [Sov. Phys. Acoust. **2**, 68 (1956)].

[32] B. Jusserand, F. Alexandre, J. Dubard, and D. Paquet, Raman scattering study of acoustical zone-center gaps in GaAs/AlAs superlattices, Phys. Rev. B **33**, 2897 (1986).

[33] M. Balkanski and R. F. Wallis, *Semiconductor Physics and Applications* (Oxford University Press, Oxford, UK, 2000).

[34] The finite spectral width of the short pump pulses leads to a distribution in k_{light}, resulting in a distribution of phonon frequencies. Even for the phonons at $2k_{\text{light}}$ this effect amounts to only 0.5 GHz, much smaller than the observed width of 7 GHz.

[35] G. Rozas, M. F. Pascual Winter, A. Fainstein, B. Jusserand, P. O. Vaccaro, S. Saravanan, and N. Saito, Piezoelectric semiconductor acoustic cavities, Phys. Rev. B **72**, 035331 (2005).

[36] H. J. Zeiger, J. Vidal, T. K. Cheng, E. P. Ippen, G. Dresselhaus, and M. S. Dresselhaus, Theory for displacive excitation of coherent phonons, Phys. Rev. B **45**, 768 (1992).

[37] M. Bargheer, N. Zhavoronkov, Y. Gritsai, J. C. Woo, D. S. Kim, M. Woerner, and T. Elsaesser, Coherent atomic motions in a nanostructure studied by femtosecond x-ray diffraction, Science **306**, 1771 (2004).

[38] M. Hase, S.-I. Nakashima, K. Mizoguchi, H. Harima, and K. Sakai, Ultrafast decay of coherent plasmon-phonon coupled modes in highly doped GaAs, Phys. Rev. B **60**, 16526 (1999).

[39] A. Huynh, B. Perrin, N. D. Lanzillotti-Kimura, B. Jusserand, A. Fainstein, and A. Lemaître, Subterahertz monochromatic acoustic wave propagation using semiconductor superlattices as transducers, Phys. Rev. B **78**, 233302 (2008).

[40] O. Matsuda and O. B. Wright, Reflection and transmission of light in multilayers perturbed by picosecond strain pulse propagation, J. Opt. Soc. Am. B **19**, 3028 (2002).

[41] M. F. Pascual-Winter, A. Fainstein, B. Jusserand, B. Perrin, and A. Lemaître, Spectral responses of phonon optical generation and detection in superlattices, Phys. Rev. B **85**, 235443 (2012).

[42] K.-H. Hellwege, *Einführung in die Festkörperphysik* (Springer, Berlin, 1976).

[43] J. S. Blakemore, Semiconducting and other major properties of gallium arsenide, J. Appl. Phys. **53**, R123 (1982).

[44] S. Adachi, GaAs, AlAs, and $Al_xGa_{1-x}As$: Material parameters for use in research and device applications, J. Appl. Phys. **58**, R1 (1985).

[45] P. Y. Yu and M. Cardona, *Fundamentals of Semiconductors* (Springer, Berlin, 1996).

[46] S. V. Gallego, J. Etxebarria, L. Elcoro, E. S. Tasci, and J. M. Perez-Matoa, Automatic calculation of symmetry-adapted tensors in magnetic and non-magnetic materials: A new tool of the Bilbao Crystallographic Server, Acta Crystallogr., Sect. A **75**, 438 (2019).

[47] C. Rauch, G. Strasser, K. Unterrainer, W. Boxleitner, E. Gornik, and A. Wacker, Transition Between Coherent and Incoherent Electron Transport in GaAs/GaAlAs Superlattices, Phys. Rev. Lett. **81**, 3495 (1998).

[48] H. Haug and S. W. Koch, *Quantum Theory of the Optical and Electronic Properties of Semiconductors* (World Scientific, Singapore, 1993).